Multimodal Methods for *In Situ* Transmission Electron Microscope

Renu Sharma, Wei-Chang Yang and Canhui Wang

National Institute of Standards and Technology, Gaithersburg, Maryland, United States

The application of transmission electron microscopy (TEM) related techniques have extended from *ex situ* nanoscale characterization of structure and chemistry of reaction products to dynamic measurements of nanostructures during reaction processes. Commercially-available modified TEM specimen holders and TEM columns (environmental scanning-transmission electron microscope or ESTEM) are being routinely employed to follow the structural and chemical changes at elevated temperatures and under controlled atmospheres. The combination of atomic-resolution images and high spatial and energy resolution has successfully revealed the functioning of catalyst nanoparticles. We have been involved in advancing technical and analytical techniques for unveiling gas-solid interactions at nanoscale.

We have incorporated a free-standing, light focusing system in the ESTEM to excite and collect vibrational and optical spectroscopies under reactive environments. This bimodal data collection enables the acquisition of vibrational spectroscopy data concurrently with electron microscopy data, (imaging, diffraction, electron energy-loss spectroscopy(EELS)), under identical environment, and expands the spatial resolution from nanoscale to microscale.[1] For example, we have collected Raman signals from $\approx 80 \ \mu m^2$ areas, while collecting atomic-resolution videos from 200 nm^2 area, during *in situ* growth of single-walled carbon nanotubes (SWCNT) at $\approx 625 \ °C$ in ≈ 0.005 Pa of C_2H_2.[2]

Recently, we have applied localized surface plasmon (LSP) resonance energy to initiate a chemical reaction at room temperature.[3] The energy barrier for most of the chemical reactions is overcome by heating the reactants in the presence of a suitable catalyst, where the thermal energy provided by heat helps in overcoming the reaction barrier that has been reduced by the adsorption of the reactant molecules on the catalyst nanoparticle surfaces. In recent years, LSP resonance energy has been used to replace the thermal energy to initiate reactions at low temperatures, even at room temperature, mimicking photocatalysis.[4,5] We leverage on the ability of high energy electrons to excite all of the LSP modes simultaneously, and provide high spatial resolution in the nanometer range to resolve the energy loss probability, measured using EELS that indicates the location-specific coupling efficiency of the electron excitation of the LSP modes at specific resonance energies on the plasmonic nanoparticle.[6] Moreover, core-loss EELS can be used to identify gas adsorption sites and solid reaction products.

We use a monochromated electron source in an environmental scanning-transmission electron microscope (ESTEM), combined with metallic nanoparticle boundary element method (MNPBEM)[7] to characterize various LSP modes and their coupling efficiency distribution within the shape and size-controlled Au and Al nanoparticles. *In situ* core-loss EELS was used to observe CO adsorption on the Au surfaces using carbon k-edge after removing the spectral contribution of environmental CO from individual pixels in a spectrum image. Low-loss EELS map from 1.8 eV to 3.8 eV showed that the electron beam position for exciting the dipole mode most ecciciently is located at the nanoprsim corner and has an energy shift in CO environment ($P_{CO} \approx 110$ Pa) that disappears after CO evacuation, indicating a change in electron density of the Au particle as CO is adsorbed and desorbed at the selective edges, respectively. Carbon deposits, detected by core-loss EELS at the cantilevered corner edge after evacuating CO, were produced from room-temperature CO disproportion ($2CO_{(g)} \rightarrow CO_{2(g)} + C_{(s)}$), mediated by the LSP resonance excited by high energy electrons on Au nanoprism, Therefore, the active sites on Au

nanoprisms, identified using EELS, are located where the preferable CO adsorption sites and the locations of maximum field amplitude superimpose.

We then apply this method to initiate the reverse reaction at room temperature. Since the reported energy range (between 2.91 eV and 3.9 eV) required for the reverse reaction to proceed is higher than the resonance energy available in Au nanoparticles, we selected Al instead. Multimode LSP resonance energies of Al nanoparticles, spanning from 2 eV and 8 eV, are simultaneously excited by high energy electrons. Suspensions of Al nanoparticles and graphite flakes, loaded on lacey carbon TEM grids, were introduced in the ESTEM column. Graphite flakes in contact with Al nanoparticles etched away in CO_2 environment under an electron flux of $\approx 9.1 \times 10^{-6}$ nA·nm^{-2}. Thickness maps (t/λ) were used to obtain the number of carbon atoms etched as a function of (a) distance away from the nanoparticle surface, (b) number of Al nanoparticles in the irradiated area, and (c) electron beam flux. The carbon etched decreased with the increasing distance away (Figure 1A) from the nanoparticle concurring with the LSPR electric field decay, and the number of carbon atoms etched increased with the number of particles and electron beam flux (Figure 1B).

A spatial variation in carbon etching around the nanoparticles was also observed due to the local field enhancement by coupled LSP resonances (hot spots) between two or more nanoparticles clusters. Thickness maps of an area of. The thickness variation, indicated by vertical bars in Figure 1D), as measured using thickness maps of a three-nanoparticle cluster show that the highest carbon etching is confined to an area close to the interface where the nanoparticles are in contact (hot spots). These examples demonstrate that the knowledge gained from low-loss and core-loss EELS measurements can be used to design catalyst-plasmonic particle combinations for selected chemical reactions.
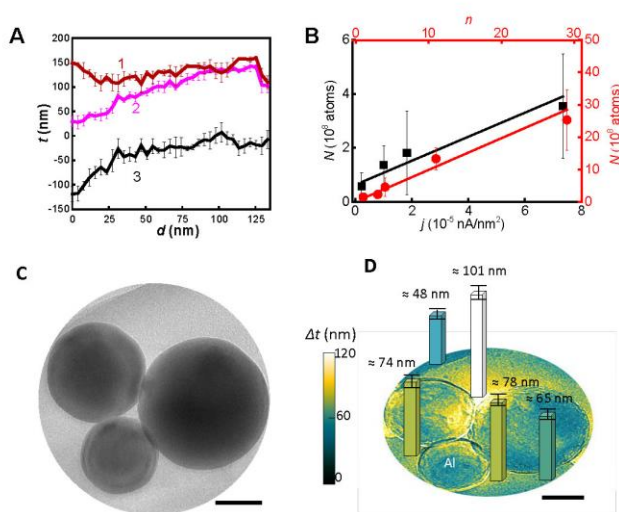

Figure 1. (A) Graphite film thickness change as a function of distance away from the surface of Al nanoparticle. (B) The number of carbon atoms etched as a function of electron flux (black) and the number of Al nanoparticles in the irradiated area (red). (C) TEM image showing a cluster of three Al particles. (D) Thickness difference map showing higher etching rate in the 'hot spot' regions (white and yellow vertical bars in the image)

References

[1] M. Picher et al., Ultramicroscopy **150** (2015) 10.

[2] M. Picher et al., Nano Letters **14**, (2014) 6104.

[3] W-C. D. Yang, Nature Materials **18** (2019), 614.

[4] S. Mukherjee, S. et al., J. American Chemical Society **136**, (2014) 64.

[5] S. Linic, U. Aslam, C. Boerigter, and M. Morabito, Nature Materials **14**, (2015) 567.

[6] Nicoletti, O. et al., Nature **502**, 80-84 (2013).

[7] U Hohenester, Computer Physics Communications **185** (2014), p. 1177.